

**Flow cytometric cell cycle analysis**

Cells were fixed in 66% methanol, treated with RNase A (100 mg ml<sup>-1</sup>) and propidium iodide (5 mg ml<sup>-1</sup>), and analysed using a FACScan apparatus (Becton Dickinson).

**Cdk2 kinase activity**

Cells were lysed in TNE buffer and 100 µg of cell extract was immunoprecipitated and analysed as described in ref. 26.

Received 22 July; accepted 16 September 2002; doi:10.1038/nature01119.

Published online 2 October 2002.

1. Vogelstein, B., Lane, D. & Levine, A. J. Surfing the p53 network. *Nature* **408**, 307–310 (2000).
2. Vousden, K. H. & Lu, X. Live or let die: the cell's response to p53. *Nature Rev. Cancer* **2**, 594–604 (2002).
3. Lane, D. How cells choose to die. *Nature* **414**, 25–27 (2001).
4. Grandori, C., Cowley, S. M., James, L. P. & Eisenman, R. N. The Myc/Max/Mad network and the transcriptional control of cell behavior. *Annu. Rev. Cell Dev. Biol.* **16**, 653–699 (2000).
5. Alexandrow, M. G., Kawabata, M., Aakre, M. & Moses, H. L. Overexpression of the c-Myc oncoprotein blocks the growth-inhibitory response but is required for the mitogenic effects of transforming growth factor beta 1. *Proc. Natl Acad. Sci. USA* **92**, 3239–3243 (1995).
6. Mitchell, K. O. & El-Deiry, W. S. Overexpression of c-Myc inhibits p21WAF1/CIP1 expression and induces S-phase entry in 12-O-tetradecanoylphorbol-13-acetate (TPA)-sensitive human cancer cells. *Cell Growth Differ.* **10**, 223–230 (1999).
7. Claassen, G. F. & Hann, S. R. A role for transcriptional repression of p21CIP1 by c-Myc in overcoming transforming growth factor-β-induced cell-cycle arrest. *Proc. Natl Acad. Sci. USA* **97**, 9498–9503 (2000).
8. Warner, B. J., Blain, S. W., Seoane, J. & Massague, J. Myc downregulation by transforming growth factor β required for activation of the p15Ink4B G1 arrest pathway. *Mol. Cell. Biol.* **19**, 5913–5922 (1999).
9. Datto, M. B., Yu, Y. & Wang, X.-F. Functional analysis of the transforming growth factor β responsive elements in WAF1/Cip1/p21 promoter. *J. Biol. Chem.* **270**, 28623–28628 (1995).
10. El-Deiry, W. S. *et al.* WAF1, a potential mediator of p53 tumour suppression. *Cell* **75**, 817–825 (1993).
11. Zeng, Y. X. & el-Deiry, W. S. Regulation of p21WAF1/CIP1 expression by p53-independent pathways. *Oncogene* **12**, 1557–1564 (1996).
12. Massague, J., Blain, S. W. & Lo, R. S. TGFβ signaling in growth control, cancer, and heritable disorders. *Cell* **103**, 295–309 (2000).
13. Zeng, Y. X., Somasundaram, K. & el-Deiry, W. S. AP2 inhibits cancer cell growth and activates p21WAF1/CIP1 expression. *Nature Genet.* **15**, 78–82 (1997).
14. Biggs, J. R., Kudlow, J. E. & Kraft, A. S. The role of the transcription factor Sp1 in regulating the expression of the WAF1/CIP1 gene in U937 leukemic cells. *J. Biol. Chem.* **271**, 901–906 (1996).
15. Waldman, T., Kinzler, K. W. & Vogelstein, B. p21 is necessary for the p53-mediated G1 arrest in human cancer cells. *Cancer Res.* **55**, 5187–5190 (1995).
16. Bunz, F. *et al.* Requirement for p53 and p21 to sustain G2 arrest after DNA damage. *Science* **282**, 1497–1501 (1998).
17. Gewirtz, D. A. A critical evaluation of the mechanisms of action proposed for the antitumor effects of the anthracycline antibiotics adriamycin and daunorubicin. *Biochem. Pharmacol.* **57**, 727–741 (1999).
18. Resnick-Silverman, L., St Clair, S., Maurer, M., Zhao, K. & Manfredi, J. J. Identification of a novel class of genomic DNA-binding sites suggests a mechanism for selectivity in target gene activation by the tumour suppressor protein p53. *Genes Dev.* **12**, 2102–2107 (1998).
19. Zawel, L. *et al.* Human Smad3 and Smad4 are sequence-specific transcription activators. *Mol. Cell* **1**, 611–617 (1998).
20. Staller, P. *et al.* Repression of p15INK4b expression by Myc through association with Miz-1. *Nature Cell Biol.* **3**, 392–399 (2001).
21. Seoane, J. *et al.* TGFβ influences Myc, Miz-1 and Smad to control the CDK inhibitor p15INK4b. *Nature Cell Biol.* **3**, 400–408 (2001).
22. Ziegelbauer, J. *et al.* Transcription factor MIZ-1 is regulated via microtubule association. *Mol. Cell* **8**, 339–349 (2001).
23. Zindy, F. *et al.* Myc signaling via the ARF tumour suppressor regulates p53-dependent apoptosis and immortalization. *Genes Dev.* **12**, 2424–2433 (1998).
24. Burri, N. *et al.* Methylation silencing and mutations of the p14ARF and p16INK4a genes in colon cancer. *Lab. Invest.* **81**, 217–229 (2001).
25. Polyak, K., Waldman, T., He, T. C., Kinzler, K. W. & Vogelstein, B. Genetic determinants of p53-induced apoptosis and growth arrest. *Genes Dev.* **10**, 1945–1952 (1996).
26. Reynisdottir, I., Polyak, K., Iavarone, A. & Massague, J. Kip/Cip and Ink4 Cdk inhibitors cooperate to induce cell cycle arrest in response to TGF-β. *Genes Dev.* **9**, 1831–1845 (1995).
27. Peukert, K. *et al.* An alternative pathway for gene regulation by Myc. *EMBO J.* **16**, 5672–5686 (1997).
28. Li, J. M., Nichols, M. A., Chandrasekharan, S., Xiong, Y. & Wang, X. F. Transforming growth factor beta activates the promoter of cyclin-dependent kinase inhibitor p15INK4B through an Sp1 consensus site. *J. Biol. Chem.* **270**, 26750–26753 (1995).
29. Hata, A. *et al.* OAZ uses distinct DNA- and protein-binding zinc fingers in separate BMP-Smad and Olf signaling pathways. *Cell* **100**, 229–240 (2000).
30. Shang, Y., Hu, X., DiRenzo, J., Lazar, M. A. & Brown, M. Cofactor dynamics and sufficiency in estrogen receptor-regulated transcription. *Cell* **103**, 843–852 (2000).

**Supplementary Information** accompanies the paper on Nature's website  
 (♦ <http://www.nature.com/nature>).

**Acknowledgements** We thank W. El-Deiry and S. Lowe for providing the recombinant adenovirus; B. Vogelstein and K. Kinzler for the HCT116 cell lines and the PUMA antibody; M. Eilers for Miz constructs; R. Tjian for the Miz-1 antibody and the bacterial expression vector encoding Miz-1; and S. Blain for advice. We also thank D. Domingo and the Memorial Sloan-Kettering flow cytometry core facility for their help in the FACS analysis. J.M. is an Investigator of the Howard Hughes Medical Institute.

**Competing interests statement** The authors declare that they have no competing financial interests.

**Correspondence** and requests for materials should be addressed to J.M.  
 (e-mail: j-massague@ski.mskcc.org).

**Tumour-derived soluble MIC ligands impair expression of NKG2D and T-cell activation**

**Veronika Groh, Jennifer Wu, Cassian Yee & Thomas Spies**

*Fred Hutchinson Cancer Research Center, Clinical Research Division, 1100 Fairview Avenue North, Seattle, Washington 98109, USA*

Engagement of the NKG2D receptor by tumour-associated ligands may promote tumour rejection by stimulating innate and adaptive lymphocyte responses<sup>1–5</sup>. In humans, NKG2D is expressed on most natural killer cells, γδ T cells and CD8αβ T cell<sup>1</sup>. Ligands of NKG2D include the major histocompatibility complex class I homologues MICA and MICB, which function as signals of cellular stress<sup>6,7</sup>. These molecules are absent from most cells and tissues but can be induced by viral and bacterial infections and are frequently expressed in epithelial tumours<sup>8–11</sup>. MIC engagement of NKG2D triggers natural killer cells and costimulates antigen-specific effector T cells<sup>1,10</sup>. Here we show that binding of MIC induces endocytosis and degradation of NKG2D. Expression of NKG2D is reduced markedly on large numbers of tumour-infiltrating and matched peripheral blood T cells from individuals with cancer. This systemic deficiency is associated with circulating tumour-derived soluble MICA, causing the downregulation of NKG2D and in turn severe impairment of the responsiveness of tumour-antigen-specific effector T cells. This mode of T-cell silencing may promote tumour immune evasion and, by inference, compromise host resistance to infections.

Ectopic expression of NKG2D ligands causes rejection of transfected tumour cells by natural killer (NK) cells and primed cytotoxic T cells in syngeneic mice<sup>2,3</sup>. Immunity is induced against subsequent challenges with tumour cells that lack NKG2D ligands<sup>3</sup>. This evidence reinforces the potential significance of human MIC–NKG2D ligand–receptor signalling in immune responses against tumours. But the presence of MIC on many progressing tumours, including breast, lung, gastric, renal, colon, ovarian and prostate carcinomas and melanomas<sup>8</sup>, suggests that MIC or NKG2D might be functionally impaired, thereby promoting immune evasion.

We examined NKG2D expression on CD8<sup>+</sup> T cells among tumour infiltrating lymphocytes (TILs) extracted from 39 epithelial tumours that were either positive or negative for MIC by monoclonal antibody staining of cell suspensions and flow cytometry. In all 13 MIC-negative tumour specimens examined, the surface amounts of NKG2D were unaltered as compared to normal control peripheral blood mononuclear cells (PBMCs; ref. 1, Fig. 1a and data not shown). By contrast, the mean fluorescence intensities of NKG2D on CD8<sup>+</sup> T cells from all 26 MIC-positive tumours tested were reduced by about 60–70% (Fig. 1b). This observation was not dependent on the proportions of MIC-positive tumour cells, which ranged from 40 to 100% (ref. 8 and data not shown). Expression of NKG2D was similarly reduced on T cells among matched PBMCs (Fig. 1b). This deficiency was not associated with T-cell subsets defined by differentiation or activation markers CD28, CCR7, CD45 isoforms and CD69. Substantially reduced expression of NKG2D was also observed on CD56<sup>+</sup> NK cells and γδ T cells (data not shown). These results showed that a systemic impairment of NKG2D is linked to the presence of tumour-associated MIC.

We examined the apparent effect of MIC on NKG2D expression by culturing normal PBMCs together with C1R-MICA (or C1R-MICB) B-cell transfectants, untransfected controls, and freshly isolated MIC-positive melanoma cells. We used conditions favouring conjugate formation, and examined the cells by three-colour

staining of dissociated cells with monoclonal antibodies against CD3, CD8 and NKG2D, and flow cytometry. After 6 h, the average amounts of surface NKG2D began to decline and reached a maximum five- to eightfold reduction between 24 and 48 h in the presence (Fig. 2a; data not shown) but not in the absence (Fig. 2b) of MIC. Similar results were obtained with melanoma-antigen-specific HLA-A2-restricted T-cell clones after co-culture with MART-1- or gp100-peptide-pulsed C1R-A2-MICA transfectants, but not with identically treated C1R-A2 cells (data not shown). These results indicate that MIC-induced downregulation of NKG2D is independent of T-cell antigen receptor (TCR) stimulation.

As many receptors undergo ligand-induced endocytosis followed by recycling or degradation<sup>12-14</sup>, we explored the fate of NKG2D by measuring its surface and total cellular amounts by using random CD8<sup>+</sup> αβ T-cell clones exposed for 12 h to C1R-MICA cells and flow cytometry. As with the surface protein, the mean fluorescence intensity reflecting the total NKG2D content of permeabilized cells was strongly reduced as compared to control T cells exposed to C1R cells (Fig. 2c). But treating T cells with bafilomycin A1 or chloroquine, which are inhibitors of lysosomal degradation, prevented this decrease in total cellular NKG2D (Fig. 2c; data not shown). Inhibition of protein synthesis with cycloheximide had no effect. Thus, at least a large proportion of endocytosed NKG2D was not recycled but degraded.

These results offered an explanation for the deficiency of NKG2D

among TILs, which directly contact MIC-positive tumour cells, but not PBMCs. We therefore considered that tumour-associated MIC might be shed into the circulation, possibly as a result of tumour cell death, secretion of exosomes or proteolysis, or a combination thereof. By a sandwich enzyme-linked immunosorbent assay (ELISA) using noncompeting solid-phase capture and biotinylated detection monoclonal antibodies 6G6 (specific for the α3 domain of MICA and MICB)<sup>7</sup> and 2C10 (specific for the MICA α1α2 domains)<sup>6</sup> respectively, we detected a minimum of 1.5 ng ml<sup>-1</sup> purified recombinant soluble MICA (rsMICA) after reaction with streptavidin-conjugated horse radish peroxidase (HRP) and tetramethyl-benzidine substrate (Fig. 3).

We obtained positive results, indicating maximum amounts of about 25–50 ng ml<sup>-1</sup> soluble MICA (sMICA), with 7 of 14 blood serum samples from individuals with tumours and a NKG2D<sup>low</sup> phenotype (2/4 breast, 3/3 lung, 0/2 ovarian and 0/1 colon tumours, and 2/4 melanomas). This incomplete correlation might be due to technical limitations including the sensitivity of the ELISA and its lack of detection of sMICB. All six samples from individuals with normal NKG2D expression gave negative results (Fig. 3). sMICA was also detected in cleared supernatants of colon (HCT-116), prostate (PC3), ovarian (HTB-79) and melanoma (375) tumour cell lines grown to high confluency, but not in supernatants of transfected B cell lines (data not shown). Thus, the shedding of MIC was a property of epithelial tumour cells. Incubation of random CD8<sup>+</sup> αβ T-cell clones for 24 h with rsMICA resulted in fivefold reductions in the mean surface quantities of NKG2D (Fig. 4a). T-cell-bound rsMICA was detected in the early incubation phase

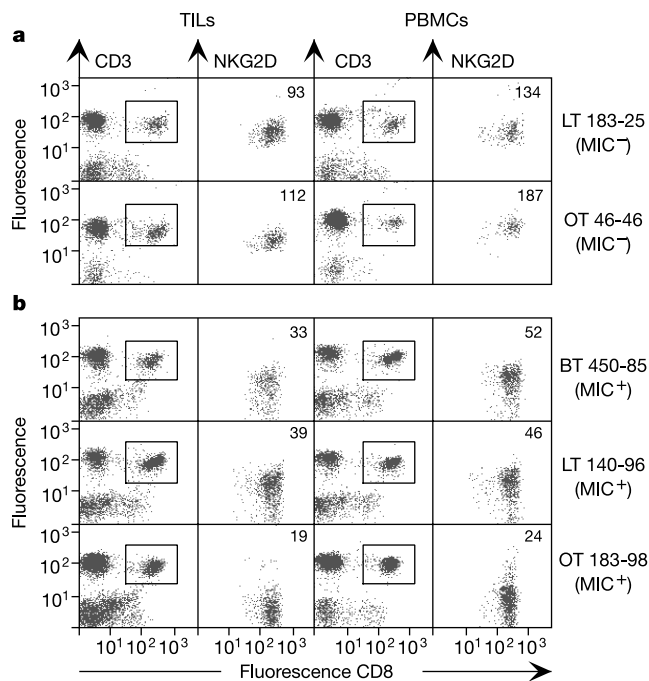


**Figure 1** Reduced expression of NKG2D on CD8<sup>+</sup> αβ T cells among TILs and PBMCs from individuals with MIC-positive tumours. **a**, Three-colour flow cytometry analysis with gating on CD3<sup>+</sup> (y axis) CD8<sup>+</sup> (x axis) T cells (dot plot columns 1 and 3) shows that the surface amounts of NKG2D (y axis; dot plot columns 2 and 4) are normal when tumours lack expression of MIC (see ref. 1 for comparison with T cells from healthy individuals). Dot plots shown are representative of 13 matched MIC-negative tumour and PBMCs samples (2 breast, 6 lung, 1 ovarian and 2 colon tumours, and 2 melanomas). **b**, Reduced expression of NKG2D among CD3<sup>+</sup>CD8<sup>+</sup> αβ T cells from TILs and PBMCs associated with MIC-positive tumours (see ref. 8 for representative tumour cell expression profiles of MIC). Dot plots shown are representative of six breast, five lung, four ovarian and three colon carcinomas, and eight melanomas. The fluorescent labels are described in Methods. Numbers in the top right corners represent the NKG2D mean fluorescence intensities derived from histograms. Tumour specimens are given on the right: BT, breast tumour; LT, lung tumour; OT, ovarian tumour.

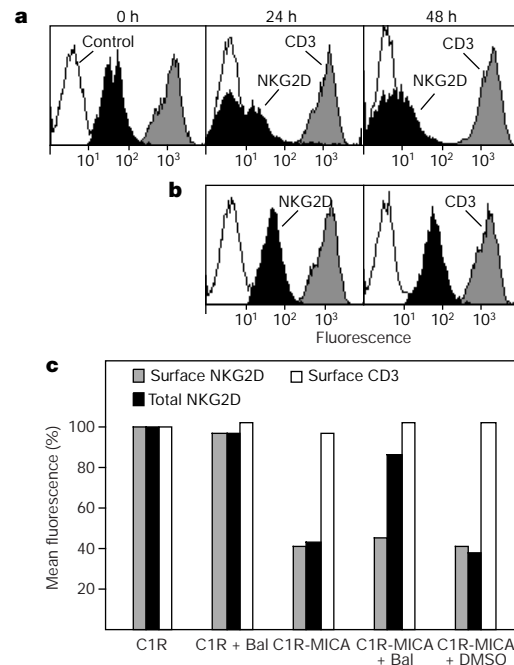


**Figure 2** MIC-induced downregulation and degradation of NKG2D. **a**, CD3<sup>+</sup>CD8<sup>+</sup> T cells among normal PBMCs show five- to eightfold reductions in the mean fluorescence intensity staining of NKG2D after co-culture with C1R-MICA transfectants. **b**, No effect is observed with untransfected C1R cells. Open profiles, IgG1 isotype control staining; shaded profiles, CD3 staining; filled profiles, NKG2D staining. **c**, Endocytosis and degradation of NKG2D. After co-culture of CD8<sup>+</sup> αβ T-cell clones derived from peripheral blood with C1R-MICA transfectants but not with C1R cells, both cell-surface and total cellular NKG2D are substantially reduced. Treating T cells with bafilomycin A1 prevents the decrease in total cellular NKG2D. The solvent control is DMSO. Surface CD3 remains unchanged. The mean fluorescence intensities obtained after exposure to negative control C1R cells are arbitrarily set as 100%. Data are representative of five independent experiments.

but not after 24 h, presumably because of degradation. Thus, rsMICA did not interfere with binding of the monoclonal antibody against NKG2D (Fig. 4a).

These results suggested that tumour-derived sMICA and presumably sMICB in peripheral blood of individuals with cancer causes the downregulation of NKG2D. This hypothesis was confirmed by experiments showing that sera from individuals with MIC-positive tumours, but not from negative controls, down-regulated NKG2D expression on CD8<sup>+</sup> T cells among normal PBMCs even when sMICA was undetectable by ELISA, and that this activity was neutralized in the presence of a monoclonal antibody specific for MIC (Fig. 5). At least in part, this capacity of sMIC may be explained by its high binding affinity for NKG2D<sup>15,16</sup>. With peripheral blood T cells, the low expression of NKG2D was reversed after 7–8 d of culture (data not shown), or more rapidly after 24 h in the presence of a monoclonal antibody against CD3. But the effect of TCR complex stimulation was suppressed by the addition of rsMICA (Fig. 4b).

Ligand engagement of NKG2D augments cytolytic responses under conditions of suboptimal T-cell activation and costimulates cytokine production and T-cell proliferation<sup>9,10</sup>. Signalling is mediated by DAP10, an adaptor protein that is associated with NKG2D<sup>17</sup>. To assess the functional impairment of NKG2D<sup>low</sup> T cells, we tested MART-1-specific T-cell clones<sup>18</sup> with rsMICA-induced low expression of NKG2D (Fig. 6a) against MIC-positive melanoma target cells pulsed with titred concentrations of the antigenic M27 peptide. Within a range of suboptimal peptide concentrations, the cytolytic responses of the NKG2D<sup>low</sup> T cells were substantially lower than those of untreated NKG2D<sup>high</sup> T cells (Fig. 6b). We also tested the responses of freshly isolated TILs (HLA-A2<sup>+</sup>) from MIC-negative and MIC-positive melanomas to specific MHC-peptide antigen and MIC stimulation. CD8<sup>+</sup> T cells purified by negative selection were stimulated for short periods with irradiated C1R-A2-MICA transfectants pulsed with M27 peptide. Antigen-specific T cells were labelled with HLA-A2-M27 tetramer<sup>18</sup> and stained for NKG2D. Fixed and permeabilized cells were stained for interferon- $\gamma$  (IFN- $\gamma$ ), which could accumulate intracellularly owing to experimental inhibition of the secretory pathway. Analysis by flow cytometry showed induction of IFN- $\gamma$  in a substantial proportion of NKG2D<sup>high</sup> (Fig. 6d) but not NKG2D<sup>low</sup> (Fig. 6c) T cells. Thus, T-cell stimulation by NKG2D was profoundly impaired.

Together, our results indicate that tumour shedding of MIC systemically impairs the responses of CD8  $\alpha\beta$  T cells and presumably NK cells, thus compromising the immunological competence

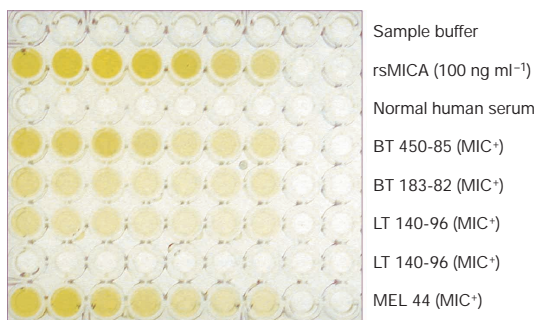


**Figure 3** Detection of sMICA by ELISA in serum samples from individuals with MIC-positive tumours and reduced expression of NKG2D. Horizontal wells from left to right are serial 1:2 dilutions of sample buffer, rsMICA (100 ng ml<sup>-1</sup>), normal human serum, four serum samples from individuals with MIC-positive tumours (BT 450-85, BT 183-82, LT 140-96 and MEL 44) and a sample from an individual with a MIC-negative tumour (LT 183-25). Results are representative of seven MIC-positive samples (two breast and three lung tumours, and two melanomas) and six MIC-positive samples (one breast and five lung tumours). BT, breast tumour; LT, lung tumour; MEL, melanoma.

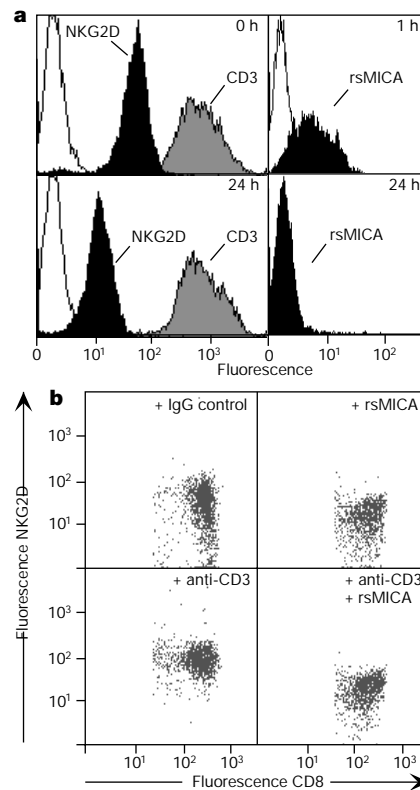


**Figure 4** Downregulation of NKG2D by rsMICA. **a**, Left, incubation of rsMICA (100 ng ml<sup>-1</sup>) with CD8<sup>+</sup>  $\alpha\beta$  T-cell clones derived from peripheral blood results in reduced surface amounts of NKG2D. A similar but less pronounced effect is induced by much lower concentrations of rsMICA (10 ng ml<sup>-1</sup>; not shown). Right, cell-associated rsMICA is detected after 1 h but not after 24 h of incubation. Open profiles, IgG1 isotype control staining. Data are representative of experiments with five different T-cell clones. **b**, Melanoma-derived TILs gated on CD3<sup>+</sup>CD8<sup>+</sup> T cells show further decreases in expression of NKG2D after incubation with rsMICA (top). NKG2D was induced by a monoclonal antibody against CD3 but not in the additional presence of rsMICA (bottom).

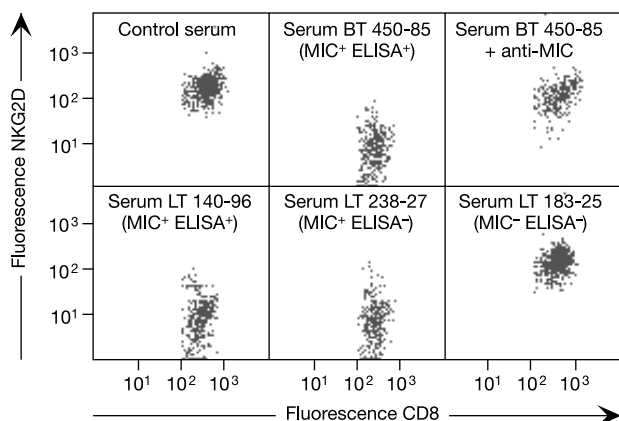


**Figure 5** Downregulation of NKG2D by sera from individuals with MIC-positive tumours. The fluorescence intensity of NKG2D measured by staining with monoclonal antibody 1D11 (ref. 1) and FITC-conjugated goat antibody against mouse IgG on CD8<sup>+</sup> T cells among normal PBMCs is markedly diminished after 24 h of incubation in 1:5 dilutions of sera from individuals with MIC-positive breast or lung tumours (BT 450-85, LT 140-96 and LT 238-27). This activity is neutralized in the presence of 6D4 monoclonal antibody against MIC<sup>7</sup> (top right plot) and is not observed with normal control serum or with serum from an individual with a MIC-negative lung tumour (LT 183-25). Note that NKG2D is downregulated by serum from an individual with a MIC-positive tumour (LT 238-27) in which sMICA is undetectable by ELISA.

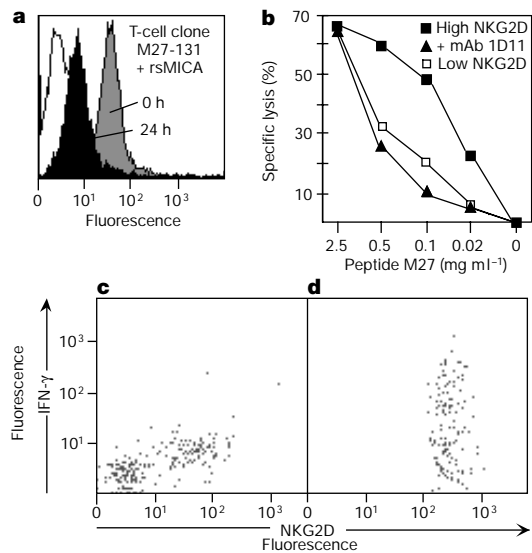


**Figure 6** Functional impairment of NKG2D<sup>low</sup> T cells. **a**, Incubation with rsMICA reduces NKG2D expression on the HLA-A2-restricted and MART-1-specific M27-131 T cells<sup>18</sup>. **b**, Under conditions of suboptimal antigen stimulation of TCR, NKG2D<sup>low</sup> M27-131 T cells respond poorly against melanoma 375 cells pulsed with titred concentrations of M27 peptide. Untreated NKG2D<sup>high</sup> M27-131 T cells show augmented cytolytic responses<sup>10</sup>. The 1D11 monoclonal antibody<sup>1</sup> is specific for NKG2D. **c**, NKG2D<sup>low</sup> CD8<sup>+</sup> αβ T cells isolated from a MIC-positive melanoma and labelled with HLA-A2-M27 tetramer show no or little induction of IFN-γ after stimulation with C1R-A2-MICA transfectants pulsed with M27 peptide. **d**, A substantial proportion of identically treated NKG2D<sup>high</sup> M27-specific T cells from a MIC-negative melanoma produce a strong IFN-γ response.

of individuals with cancer. Although expression of MIC by nascent tumours might, to some extent, be effective in mobilizing responses from effector T cells and NK cells, its shedding at progressive stages of tumour growth probably promotes immune evasion. Notably, the factors that determine the tumour-associated expression of MIC and the shedding mechanism remain to be defined. But monitoring the presence of sMICA in tissue or peripheral blood samples might be applicable to the prognosis or diagnosis of cancer, just as the MIC-NKG2D system might offer possibilities for therapy. □

**Methods**

**Tumour specimens and PBMCs**

Specimens of 8 breast, 11 lung, 5 ovarian and 5 colon carcinomas and of 10 melanomas from diagnostic or therapeutic resections and matched peripheral blood samples were a gift from H. Secrist and D. Byrd and R. Yeung. Tumours were diagnosed by histopathological criteria. We obtained normal PBMCs from random healthy volunteers. These activities were approved by local institutional review boards and all subjects gave written informed consent. We prepared TILs and tumour cell suspensions as described<sup>8</sup>. PBMCs were purified by Ficoll/Hypaque density centrifugation.

**Antibodies and flow cytometry**

We stained suspensions of tumour cells with monoclonal antibody 6D4 (against MICA and MICB)<sup>7</sup> and phycoerythrin (PE)-conjugated goat antibodies against mouse F(ab')<sub>2</sub> (Southern Biotechnologies), and analysed them using a FACScan (Beckton Dickinson) flow cytometer. TILs and PBMCs were examined by three-colour flow cytometry using various combinations of antibodies against CD3, CD4, CD8, CD56, TCRγδ, CD28, CD69, CCR7, CD45RO and CD45RA conjugated to PE, fluorescein isothiocyanate (FITC), PerCP or allophycocyanin (BD/PharMingen). We detected binding of the 1D11 monoclonal antibody against NKG2D (ref. 1) to TILs, PBMCs and T-cell clones with PE- or FITC-conjugated goat antibodies against mouse F(ab')<sub>2</sub>.

**Modulation of NKG2D**

Freshly isolated PBMCs were co-cultured with irradiated C1R-MICA transfectants, C1R cells or freshly isolated MIC-positive melanoma cells (at 1:2 ratios) after a brief low-speed centrifugation in round-bottom microtitre plates. After various durations, the cells were washed in PBS plus 0.5% EDTA and stained for expression of CD3, CD8 and NKG2D. We gated transfectants, C1R and tumour cells using forward- and side-scatter parameters. Similarly, HLA-A2-restricted CD8 αβ T-cell clones specific for MART-1 (M27 peptide AAGIGILTIV)<sup>18</sup> or gp100 (G154 peptide KTGWQYVQV)<sup>18</sup> were cultured together with

C1R-A2-MICA or C1R-A2 transfectants pulsed with optimal concentrations (2.5 μg ml<sup>-1</sup>) of the appropriate peptide.

We showed ligand-induced endocytosis and degradation of NKG2D with random CD8<sup>+</sup> αβ T-cell clones that were established as described<sup>1</sup>. We cultured T cells for 12 h with C1R-MICA or C1R control cells, washed them and fixed them with paraformaldehyde. Half of the cells were stained for surface CD3, CD8 and NKG2D; the other half were stained after permeabilization in 0.1% saponin. Continuous exposure of T cells to bafilomycin A1 (Sigma; 0.5 μM) or chloroquine (33 μM) was used to inhibit lysosomal degradation. We used dimethyl sulphoxide (DMSO; 1%) as the solvent control<sup>14</sup>.

Downregulation of NKG2D by rsMICA was shown by incubating random CD8 αβ T-cell clones with rsMICA (10 or 100 ng ml<sup>-1</sup>) for various durations before flow cytometry analysis of surface NKG2D. Surface-associated rsMICA was monitored with monoclonal antibody 2C10 (ref. 6). NKG2D<sup>low</sup> TILs extracted from a MIC-positive melanoma were used for induction of NKG2D by a plate-bound antibody against CD3 (50 ng ml<sup>-1</sup>) after 24 h of incubation. Induction was prevented by rsMICA (100 ng ml<sup>-1</sup>). Downregulation of NKG2D by sera from individuals with MIC-positive tumours was shown by incubation of freshly isolated normal PBMCs with 1:5 dilutions of sera (BT 450-85, LT 140-96 and LT 238-27) for 24 h before flow cytometry analysis. Normal serum and serum from an individual with a MIC-negative lung tumour (LT 183-25) were used as negative controls.

**ELISA and rsMICA**

High-binding EIA/RIA polystyrene plates (Corning) were coated with capture 6G6 monoclonal antibody (10 μg ml<sup>-1</sup> PBS, 50 μl per well) for 10 h at 4 °C, washed with PBS plus 0.1% Tween 20, blocked overnight at 4 °C with blocking buffer (215 μl of 20 mM Tris-OH, pH 7.5, 150 mM NaCl, 5% EIA grade bovine serum albumin (BSA) and 0.05% Tween 20), and washed with PBS plus 0.1% Tween 20. Serial 1:2 dilutions in sample buffer (blocking buffer containing 0.1% BSA and 0.1% Tween 20) of rsMICA and patient and control serum samples were plated at 50 μl per well, incubated for 2 h at room temperature on a shaker and washed five times in PBS plus 0.1% Tween 20. After incubation under the same conditions with 50 μl of biotinylated 2C10 detection monoclonal antibody (1.2 μg ml<sup>-1</sup> sample buffer), washed plates were incubated for 30 min at room temperature with 50 μl of streptavidin-HRP (Vector Laboratories), washed and reacted for 7–8 min with tetramethyl-benzidine (Kirkegaard and Perry Laboratories). We stopped the reactions with 1 M phosphoric acid (100 μl per well) and scored them at a wavelength of 450 nm using a Veramax microplate reader (Molecular Devices).

rsMICA was expressed as a secreted protein in High-Five insect cells (Invitrogen) using the BAC-TO-BAC Baculovirus expression system (GibcoBRL)<sup>15</sup>. The extracellular sequences of MICA corresponding to the signal peptide and the α1α2α3 domains were amplified from template complementary DNA, using oligonucleotide primers and PCR, and purified. In subsequent rounds of PCR and amplicon purification, the truncated MICA sequence was fused to a 15-residue biotinylation recognition sequence<sup>19</sup>, which was not used in this study, using the primers 5'-TCTGGATCCATGGGGCTGGGCCGGTC-3' (MICA 5' end) and 5'-ACGATGAATCCACACCATTTTCTGTGCATCCAGAATATGATG CAGGCTTCCTTCCAGAGGGGACAGGGGTAG-3' (biotinylation recognition sequence/glycine-serine linker/MICA 3'-end overlap), and to sequences for a hexahistidine tract and the eight-amino-acid Flag tag (DYKDDDDK) M2 antibody epitope<sup>20</sup>. The amplicon was flanked by restriction sites for insertion into pFASTBAC1 (GibcoBRL). We transfected the sequenced construct into Sf9 cells for production of high-titre recombinant Baculovirus, which was used to infect High-Five cells. Media were collected from cell cultures grown in spinner flasks 4–5 d after infection, cleared, filtered and applied to a Ni<sup>2+</sup>-charged Chelating Sepharose Fast Flow resin column (Pharmacia). Recombinant protein was eluted with imidazol in PIPES, NaCl, Na<sub>3</sub> buffer, further purified by Superdex S75 gel filtration chromatography (Pharmacia)<sup>15</sup>, and concentrated using a BIOMAX-100K (Millipore) ultrafiltration device. rsMICA was a monomeric protein as judged by SDS-PAGE.

**T-cell function assays**

We cultured HLA-A2-restricted and MART-1-specific M27-131 T cells<sup>18</sup> for 24 h with 100 ng ml<sup>-1</sup> rsMICA to induce low expression of NKG2D, washed them in culture media and then tested them in standard <sup>51</sup>Cr-release assays against MIC-positive melanoma 375 cells (American Type Culture Collection) that had been pulsed with titred concentrations of M27 peptide. Induction of intracellular IFN-γ was carried-out with CD8<sup>+</sup> αβ T cells obtained by negative selection with RosetteSep (StemCell Technologies) from TILs isolated from MIC-positive and MIC-negative melanomas. We stimulated T cells for 4 h with equal numbers of C1R-A2-MICA transfectants pulsed with M27 peptide in the presence of monensin (Golgistop, PharMingen) as described<sup>10</sup>. M27-specific T cells were identified with PE-conjugated HLA-A2-M27 tetramer<sup>18</sup> and stained for NKG2D. After being fixed and permeabilized by a Cytotfix/Cytoperm Plus kit (PharMingen), T cells were stained for intracellular IFN-γ with a specific allophycocyanin-conjugated monoclonal antibody (PharMingen) and analysed by flow cytometry<sup>10</sup>.

Received 24 May; accepted 8 August 2002; doi:10.1038/nature01112.

1. Bauer, S. *et al.* Activation of NK cells and T cells by NKG2D, a receptor for stress-inducible MICA. *Science* **285**, 727–729 (1999).
2. Cerwenka, A., Baron, J. L. & Lanier, L. L. Ectopic expression of retinoic acid early inducible-1 gene (RAE-1) permits natural killer cell-mediated rejection of a MHC class I-bearing tumour *in vivo*. *Proc. Natl Acad. Sci. USA* **98**, 11521–11526 (2001).
3. Diefenbach, A., Jensen, E. R., Jamieson, A. M. & Raulet, D. H. Rae1 and H60 ligands of the NKG2D receptor stimulate tumour immunity. *Nature* **413**, 165–171 (2001).
4. Long, E. O. Tumor cell recognition by natural killer cells. *Semin. Cancer Biol.* **12**, 57–61 (2002).
5. Pardoll, D. M. Stress, NK receptors, and immune surveillance. *Science* **294**, 534–536 (2002).
6. Groh, V. *et al.* Cell stress-regulated human major histocompatibility complex class I gene expressed in gastrointestinal epithelium. *Proc. Natl Acad. Sci. USA* **93**, 12445–12450 (1996).

7. Groh, V., Steinle, A., Bauer, S. & Spies, T. Recognition of stress-induced MHC molecules by intestinal epithelial  $\gamma\delta$  T cells. *Science* **279**, 1737–1740 (1998).
8. Groh, V. *et al.* Broad tumour-associated expression and recognition by tumour-derived  $\gamma\delta$  T cells of MICA and MICB. *Proc. Natl Acad. Sci. USA* **96**, 6879–6884 (1999).
9. Das, H. *et al.* MICA engagement by human V $\gamma$ 2V $\delta$ 2 T cells enhances their antigen-dependent effector function. *Immunity* **15**, 83–93 (2001).
10. Groh, V. *et al.* Costimulation of CD8  $\alpha\beta$  T cells by NKG2D *via* engagement by MIC induced on virus-infected cells. *Nature Immunol.* **2**, 255–260 (2001).
11. Tieng, V. *et al.* Binding of *Escherichia coli* adhesin AfaE to CD55 triggers cell-surface expression of the MHC class I-related molecule MICA. *Proc. Natl Acad. Sci. USA* **99**, 2977–2982 (2002).
12. Linsley, P. S., Bradshaw, J., Urnes, M., Grosmaire, L. & Ledbetter, J. A. CD28 engagement by B7/BB-1 induces transient down-modulation of CD28 synthesis and prolonged unresponsiveness to CD28 signaling. *J. Immunol.* **150**, 3161–3169 (1993).
13. Valitutti, S., Muller, S., Salio, M. & Lanzavecchia, A. Degradation of T cell receptor (TCR)–CD3- $\zeta$  complexes after antigenic stimulation. *J. Exp. Med.* **185**, 1859–1864 (1997).
14. Huard, B. & Karlsson, L. KIR expression on self-reactive CD8<sup>+</sup> T cells is controlled by T-cell receptor engagement. *Nature* **403**, 325–328 (2000).
15. Li, P. *et al.* Complex structure of the activating immunoreceptor NKG2D and its MHC class I-like ligand MICA. *Nature Immunol.* **2**, 443–451 (2001).
16. Steinle, A. *et al.* Interactions of human NKG2D with its ligands MICA and MICB and homologs of the mouse RAE-1 protein family. *Immunogenetics* **53**, 279–287 (2001).
17. Wu, J. *et al.* An activating immunoreceptor complex formed by NKG2D and DAP10. *Science* **285**, 730–732 (1999).
18. Yee, C., Savage, P. A., Lee, P. P., Davis, M. M. & Greenberg, P. D. Isolation of high avidity melanoma-reactive CTL from heterogeneous populations using peptide-MHC tetramers. *J. Immunol.* **162**, 2227–2234 (1999).
19. Schatz, P. J. Use of peptide libraries to map the substrate specificity of a peptide-modifying enzyme: A 13 residue consensus peptide specifies biotinylation in *Escherichia coli*. *Biotechnology* **11**, 1138–1143 (1993).
20. Knappik, A. & Pluckthun, A. An improved affinity tag based on the FLAG peptide for detection and purification of recombinant antibody fragments. *Biotechniques* **17**, 754–761 (1994).

**Acknowledgements** We thank R. Rhinehart and K. Kenyon for technical assistance; H. Secrist, D. Byrd and R. Yeung for tissue materials; and S. Riddell for critically reading the manuscript. This work was supported by grants from the NIH.

**Competing interests statement** The authors declare that they have no competing financial interests.

**Correspondence** and requests for materials should be addressed to V.G. (e-mail: vgroh@fhcr.org).

## A transcription-factor-binding surface of coactivator p300 is required for haematopoiesis

Lawryn H. Kasper\*, Fayçal Boussouar\*, Paul A. Ney\*, Carl W. Jackson†, Jerold Rehg‡, Jan M. van Deursen§ & Paul K. Brindle\*

\* Department of Biochemistry and † Division of Experimental Hematology; and ‡ Department of Pathology, St Jude Children’s Research Hospital, 332 North Lauderdale, Memphis, Tennessee 38105, USA  
§ Department of Pediatric and Adolescent Medicine, Mayo Clinic, Rochester, Minnesota 55905, USA

The coactivators CBP (Cre-element binding protein (CREB)-binding protein) and its paralogue p300 are thought to supply adaptor molecule and protein acetyltransferase functions to many transcription factors that regulate gene expression<sup>1</sup>. Normal development requires CBP and p300, and mutations in these genes are found in haematopoietic and epithelial tumours<sup>2–6</sup>. It is unclear, however, which functions of CBP and p300 are essential *in vivo*. Here we show that the protein-binding KIX domains of CBP and p300 have nonredundant functions in mice. In mice homozygous for point mutations in the KIX domain of p300 designed to disrupt the binding surface for the transcription factors c-Myb and CREB<sup>7–9</sup>, multilineage defects occur in haematopoiesis, including anaemia, B-cell deficiency, thymic hypoplasia, megakaryocytosis and thrombocytosis. By contrast, mice homozygous for identical mutations in the KIX domain of CBP

are essentially normal. There is a synergistic genetic interaction between mutations in c-Myb and mutations in the KIX domain of p300, which suggests that the binding of c-Myb to this domain of p300 is crucial for the development and function of megakaryocytes. Thus, conserved domains in two highly related coactivators have contrasting roles in haematopoiesis.

The KIX domain is one of several domains in CBP (also known as Crebbp) and p300 that bind transcriptional regulators (Fig. 1a); it is highly conserved in evolution, with 90% identity in human CBP and p300 (Fig. 1b). The three-dimensional structure of the CBP KIX domain in a complex containing a portion of the CREB activation domain has been determined (ref. 9 and Fig. 1c). Specific hydrophobic residues on the surface of the KIX domain are important for binding the  $\alpha$ -helical activation domains of CREB and c-Myb<sup>7,8</sup>.

We tested the role of the KIX domain transcription factor-binding surface *in vivo* by mutating three highly conserved residues that lie on one face of the  $\alpha$ 3 helix in the KIX domain of CBP (Fig. 1b, c): Tyr 650 forms part of the hydrophobic surface that makes crucial contacts with CREB; the small side chain of Ala 654 allows the close packing of CREB; and Tyr 658 forms hydrophobic interactions with CREB and forms hydrogen bonds with phosphorylated Ser 133 of CREB<sup>9</sup>. Thus, we thought that replacing Tyr 650 and Tyr 658 with alanines should disrupt bonding with CREB, and replacing the Ala 654 methyl group with a bulkier glutamine side chain should sterically hinder CREB binding. Accordingly, the individual mutations of Tyr650Ala, Ala654Gln, and Tyr658Ala each diminish CREB and c-Myb binding to KIX (refs 7, 8, and data not shown). Structure prediction analyses using AGADIR and PSIPRED predicted that KIX secondary structure would not be affected by a Tyr650Ala, Ala654Gln, Tyr658Ala triple mutation (refs 10, 11, and data not shown).

We introduced this triple mutation into the CBP and p300 loci of embryonic stem (ES) cells by homologous recombination (Fig. 1d, e). For p300, the corresponding residues, Tyr 630, Ala 634 and Tyr 638, were mutated. Correctly targeted ES cells were used to produce mice carrying mutant alleles of the KIX domain of CBP (designated *CBP*<sup>KIX</sup>) or p300 (designated *p300*<sup>KIX</sup>; Fig. 1d, e). *CBP*<sup>KIX/KIX</sup> and *p300*<sup>KIX/KIX</sup> homozygous mice were viable, although some died of unknown causes before they were 3 weeks old (mostly *p300*<sup>KIX/KIX</sup> mice; see Supplementary Information). Surviving 4-week-old *p300*<sup>KIX/KIX</sup> mice averaged about 50–70% of the size of wild-type or heterozygous littermates, and *CBP*<sup>KIX/KIX</sup> mice also tended to be smaller than their littermate controls. Analysis of the surviving *CBP*<sup>KIX/KIX</sup> mice was unrevealing apart from a slight reduction in thymocyte numbers (Supplementary Information). By contrast, *p300*<sup>KIX/KIX</sup> mice had a marked reduction in thymocyte numbers (~5% of wild type) and severe anaemia (haematocrit 20.2 ± 5.3 versus 42.3 ± 1.4% for wild type) and thrombocytosis ((5.0 ± 1.1) × 10<sup>9</sup> versus (1.2 ± 0.2) × 10<sup>9</sup> platelets per ml for wild type). Numbers of neutrophils were generally in the normal range (data not shown). The blood from *p300*<sup>KIX/KIX</sup> mice showed increased variation in erythrocyte size (compare Fig. 2b with Fig. 2a, c) and the presence of megathrombocytes (Fig. 2b, broken arrow). *CBP*<sup>+KIX</sup> and *p300*<sup>+KIX</sup> mice were essentially normal (except for a small increase in platelets in *p300*<sup>+KIX</sup> mice), which showed that the mutations were not overtly dominant (Supplementary Information).

The bone marrow of *p300*<sup>KIX/KIX</sup> mice showed megakaryocytic hyperplasia with a corresponding decrease in other bone marrow elements (compare Fig. 2d with Fig. 2e). Megakaryocytosis was evident in the spleens of these mice (compare Fig. 2g with Fig. 2f, h) and was indicated further by widespread staining for acetylcholinesterase enzyme (compare Fig. 2j with Fig. 2i) and factor VIII (data not shown). Megakaryocytosis in *p300*<sup>KIX/KIX</sup> mice was also indicated by flow cytometric analysis of bone marrow and spleen cells, which contained an overabundance of CD41-positive cells as compared with *CBP*<sup>KIX/KIX</sup> and wild-type mice (Fig. 2k). Serum